Available online at www.sciencedirect.com
SCIENCE DIRECT
Journal of Photochemistry and Photobiology A: Chemistry 181 (2006) 79–85
Journal of Photochemistry and Photobiology A:Chemistry
www.elsevier.com/locate/jphotochem

Photostabilities of novel heptamethine 3*H*-indolenine cyanine dyes with different *N*-substituents

Xiuying Chen, Xiaojun Peng *, Aijun Cui, Bingshuai Wang, Li Wang, Rong Zhang

State Key Laboratory of Fine Chemicals, Dalian University of Technology, 158 Zhongshan Road, Dalian 116012, PR China

Received 24 August 2005; received in revised form 16 October 2005; accepted 8 November 2005
Available online 15 December 2005

Abstract

Novel near-infrared (NIR) 3*H*-indocyanine dyes with different *N*-substituents were synthesized and tested to make clear the relationship between photophysical properties and structures and develop potential NIR cyanine dyes with high photostability for fluorescent imaging technology. The electron-withdrawing ability of the substituents on *N*-position of 3*H*-indolenine strongly affects the photostabilities of the NIR cyanine dyes and introducing of the electron-donating groups is favorable to obtain NIR cyanine dyes with improved photochemical stability.

Keywords: Near-infrared cyanine dye; Photostability; Fluorescence quantum yield; Photobleaching; Fluorescence labeling

1. Introduction

Recently, near-infrared (NIR) fluorescence (λ_{max}: 700–900 nm) has been applied to image various biological events in vivo [1,2]. The advantages of NIR fluorescence are the excellent penetrating ability through tissue as little NIR absorption and emission exist in natural biosystem, and the great decrease in autofluorescence, which is always encountered in visible light excitation [3]. So NIR fluorescence imaging is expected to have a major impact on biotechnology and medicine research with high sensitivity when it is incorporated in different reporter probes, including diagnosis of disease [4], labeling of proteins [5], DNA sequencing [6] and molecular recognition [7]. Cyanine dye is an excellent kind of NIR fluorophore with large molar extinction coefficients and broad wavelength tunablility. The spectra of cyanine dyes depend primarily on the length of the polymethine chain linking the two aromatic rings. The wavelengths of the excitation and emission maxima shift bathochromically by ca. 100 nm with every vinylene unit. However, along with the red shift of the wavelength, the photostability of the dyes decreases obviously. The tendency to undergo photodegradation becomes the common problem encountered by NIR cyanine dyes ($\lambda_{max} > 700$ nm) [8]. It is a key point not only to the laser-induced fluorescence imaging technology but, also, to all the practical applications involving the fluorescence spectroscopy, where either high sensitivity or high signal rate is crucial. Early analyses of the structure–property relationship of substituted trimethine dyes in benzene solution demonstrated a sensitive dependence of the photophysical properties on the substituents on the aryl rings [9]. Continuous research focus on the effects of the changes of the substituted polymethine chains [10], substituted terminal aromatic rings [11] and the scaffold of the dyes [12]. Pantonay has found that the fixed conformation enhances the photochemical and photophysical stabilities [13,14] of NIR cyanine dyes. Recently, we have reported that the central chlorine atom at cyclohexenylene-chain substituted by electron-donor group can enhance the photostability of the dyes obviously [15]. In this paper, we firstly report the great effect of *N*-substitution of 3*H*-indolenine on the photostabilities of the dyes: electron-donating groups on the N-atom of 3*H*-indolenine rings are favorable to obtain greater resistance to photobleaching than electron-withdrawing groups (Fig. 1).

2. Experiments

2.1. Characteristics of the dyes

^{1}H NMR spectra were recorded on a VARIAN 400 MHz NMR spectrometer. Electronic absorption spectra were obtained

* Corresponding author. Tel.: +86 411 88993899.
E-mail address: pengxj@dlut.edu.cn (X. Peng).

1010-6030/$ – see front matter © 2005 Elsevier B.V. All rights reserved.
doi:10.1016/j.jphotochem.2005.11.004

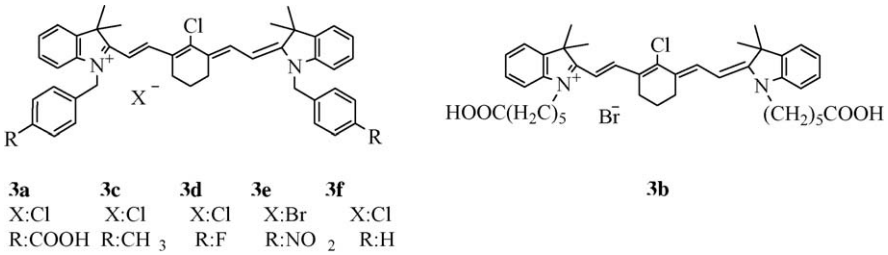

3a	3c	3d	3e	3f
X:Cl	X:Cl	X:Cl	X:Br	X:Cl
R:COOH	R:CH_3	R:F	R:NO_2	R:H

3b

Fig. 1. Structures of the NIR cyanine dyes.

on a HP-8453 spectrophotometer. Fluorescence measurements were performed on a PTI-C-700 Felix and Time-Master system. HRMS data were obtained on MICROMASS HPLC-Q-TOF MS instrument. The redox potential was measured on BAS 100B electorchemical analyzer. A three-electrode cell was composed of a glass carbon as working electrode, a platinum wire as counter electrode, and Ag/Ag^+ as reference electrode (0.01 M $AgNO_3$). The supporting electrolyte was $TBAPF_6$ (0.1 M tetra-*n*-butylammonium hexafluorophosphate) and the concentration of the dyes was 10^{-3} M in CH_3CN. All the chemicals used for the experiments were of analytical grade.

The corresponding fluorescence quantum yields were calculated relative to a standard solution of NIR larser dye IR-125 (from Aldrich Company) in DMSO ($\Phi = 0.13$) [16] and was determined using the model:

$$\Phi_x = \Phi_s \left(\frac{A_s}{A_x}\right)\left(\frac{F_x}{F_s}\right)\left(\frac{n_x}{n_s}\right)^2$$

where Φ is the fluorescence quantum yield, A the absorbance, F the area under the emission curve, and n is the refractive index of the solvents used in measurement [17]. The subscript s and x represent for the standard dye (IR125) and the tested dye, respectively.

2.2. Photofading

The photofading were carried out in quartz cells (1 cm in width) where sample solution was irradiated with a 500 W I-W lamp at room temperature. In order to eliminate the heat and the absorbance of short wavelength light, a cold trap (10 L solution of 50 g/L $NaNO_2$ and 20 cm in length) was set up between the cells and the lamp. The distance between the cells and the lamp was 25 cm. The irreversible bleaching of the dyes at the absorption peak was monitored as a function of time.

2.3. Synthesis

The synthesis routes were shown in Scheme 1. 2,3,3-Trimethyl-3*H*-indolenine (**1**) [18], 2-chloro-1-formyl-3-hydroxymethylene cyclohexene [19], and dye **3f** [20] were synthesized according to the previous procedure, respectively. **3f**: ^1H NMR (d_6-DMSO): δ 1.72 (s, 14H, $C(CH_3)_2$, CH_2), 2.50 (m, 4H, CH_2), 5.53 (s, 4H, NCH_2), 6.43 (d, $J = 14$ Hz, 2H, CH), 7.28 (m, 16H, Ar–H), 7.67 (d, 2H, $J = 7.6$ Hz, Ar–H), 8.24 (d, 2H, $J = 14$ Hz, CH). MS, *m/z*: 635.3 (M^+).

2.3.1. 1-(4-Carboxyl)benzyl-2,3,3-trimethyl-3H-indolenium (*2a*)

A 1.59 g (10 mmol) of 2,3,3-trimethyl-3*H*-indolenine (**1**) and 1.80 g (10.1 mmol) of *p*-chloromethyl benzoic acid were added into 25 mL flask containing 10 mL of 1,2-dichlorobenzene under argon. After heating the mixture at 110 °C for 12 h, the precipitate was filtered and washed with acetone. A 1.90 g of rose pink powder was obtained with no further purification, and the crude yield was 58%.

2.3.2. 1-(5-Carboxypentyl)-2,3,3-trimethyl-3H indolenium (*2b*)

2,3,3-Trimethyl-3*H* indolenine (**1**) 3.80 g (23 mmol) and 6-bromohexanoic acid 4.60 g (23 mmol) were mixed in 15 mL of

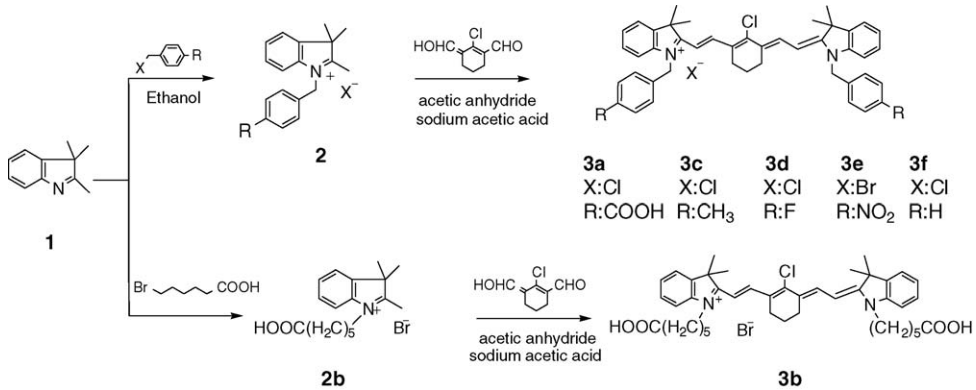

3a	3c	3d	3e	3f
X:Cl	X:Cl	X:Cl	X:Br	X:Cl
R:COOH	R:CH_3	R:F	R:NO_2	R:H

Scheme 1. Synthesis of the NIR dyes.

1,2-dichlorobenzene and heated at 110 °C for 12 h under argon in 50 mL flask. The mixture was cooled. The precipitate was filtered and washed by acetic ether. The ultimate compound (3.12 g) as pink powder was obtained for the next reaction without further purification in 39% yield.

2.3.3. 1-(4-Methyl)benzyl-2,3,3-trimethyl-3H-indolenium (2c)

A mixture of 2,3,3-trimethyl-3*H*-indolenine (**1**) (3.20 g, 20 mmol) and 4-methylbenzyl chloride (11 g, 80 mmol) was heated in 30 mL of ethanol at 80 °C for 24 h under argon. The mixture was cooled and the solvents were evaporated under vacuum. The yellow solid was crystallized from the residual solution after staying for a few days (25% yield) and, then, filtered to be used for the next reaction without further purification.

2.3.4. 1-(4-Fluoro)benzyl-2,3,3-trimethyl-3H-indolenium (2d)

In a 50 mL round-bottomed flask were placed 3.20 g (20 mmol) of 2,3,3-trimethyl-3*H*-indolenine (**1**), 11 g (80 mmol) of 4-fluoricbenzyl chloride and 30 mL of ethanol. The mixture was heated at 80 °C for 24 h under argon and, then, was cooled. After evaporated under vacuum, the solvents were removed partially and the precipitate was filtered and recrystallized in methanol. The total product (1.88 g) as yellow solid was obtained in 30% yield.

2.3.5. 1-(4-Nitro)benzyl-2,3,3-trimethyl-3H-indolenium (2e)

A mixture of 2,3,3-trimethyl-3*H*-indolenine (**1**) (3.20 g, 20 mmol) and 4-nitrobenzyl bromide (4.32 g, 20 mmol) were heated in 10 mL of 1,2-dichlorobenzene at 110 °C for 24 h under argon. The mixture was cooled and the precipitate was filtered. The solid was washed with acetone, and the total compound (2.82 g) as pink powders were prepared in 35% yield for the next reaction without further purifying.

2.3.6. Dye 3a

The intermediate **2a** (0.658 g, 2 mmol), 2-chloro-1-formyl-3-hydroxymethylene cyclohexene (0.18 g, 1 mmol) and sodium acetate (0.188 g, 2.1 mmol) were heated in 15 mL of acetic anhydride at 70 °C for 15 min. The green solution was cooled and, then, poured into saturated solution of sodium chloride. The green solid was filtered and collected. The crude product was recrystallized in acetone. The final product (0.25 g) as green powder was obtained in 30% yield. **3a**: ^{1}H NMR (d_6-DMSO): δ 1.73 (s, 14H, $C(CH_3)_2$, CH_2), 2.50 (m, 4H, CH_2), 5.62 (s, 4H, NCH_2), 6.34 (d, 2H, J = 14 Hz, CH), 7.30–7.40 (m, 5H, Ar–H), 7.67 (d, 2H, J = 7.6 Hz, Ar–H), 7.93 (d, 4H, J = 8 Hz, Ar–H), 8.24 (d, 2H, J = 14 Hz, CH). IR: 1702.04 (C=O), 1611.81 (CH=CH). High resolution MS, *m/z*: calc. 723.2990 $[M-Cl]^+$, measured 723.3008 $[M-Cl]^+$.

2.3.7. Dye 3b

2b (0.5 g, 1.4 mmol), 2-chloro-1-formyl-3-hydroxymethylene cyclohexene (0.122 g, 0.7 mmol) and sodium acetate (0.12 g, 1.41 mmol) were heated in 13 mL of acetic anhydride at 70 °C for 40 min. The green solution was cooled and, then, poured into saturated solution of sodium bromide. The green solid was filtered and collected. The pure product (0.28 g) was obtained in 52% yield by the purification on silica gel column (ethyl acetate and ethanol 1:1). ^{1}H NMR ($CDCl_3$): δ 1.53 (m, 4H, γ-CH_2(COOH)), 1.70 (s, 12H, CH_3), 1.76 (m, 4H, βCH_2), 1.84 (m, 4H, δCH_2), 2.00 (s, 2H, CH_2), 2.39 (s, 4H, αCH_2), 2.70 (s, 4H, CH_2CH=), 4.05 (t, 4H, N–CH_2), 6.16 (d, 2H, CH=CH), 7.14–7.40 (m, 8H, Ar–H), 8.31 (d, 2H, CH=CH). High resolution MS, *m/z*: calc. 683.3616 $[M-Br]^+$, measured 683.3629 $[M-Br]^+$.

2.3.8. Dye 3c

2c (1.2 g, 4 mmol), 2-chloro-1-formyl-3-hydroxymethylene cyclohexene (0.34 g, 2 mmol) and sodium acetate (0.328 g, 4 mmol) were heated in 25 mL of acetic anhydride at 70 °C for 20 min. The green solution was cooled and, then, poured into saturated solution of sodium chloride. The green solid was filtered and collected. The crude product was recrystallized from ethanol. Green powder of **3c** (0.43 g) was obtained in 31% yield. ^{1}H NMR (d_6-DMSO): δ 1.70 (s, 12H, CH_3), 1.77 (m, 2H, CH_2), 2.27 (s, 6H, CH_3), 2.56 (t, 4H, CH_2), 5.47 (s, 4H, NCH_2), 6.38 (d, 2H, J = 14.4 Hz, CH), 7.18–7.67 (m, 16H, Ar–H), 8.23 (d, 2H, J = 14.4 Hz, CH). High resolution MS, *m/z*: calc. 663.3506 $[M-Cl]^+$, measured 663.3508 $[M-Cl]^+$.

2.3.9. Dye 3d

2d (1.66 g, 5.5 mmol), 2-chloro-1-formyl-3-hydroxymethylene cyclohexene (0.46 g, 2.7 mmol) and sodium acetate (0.451 g, 5.5 mmol) were heated in 30 mL of acetic anhydride at 70 °C for 20 min. The green solution was cooled and, then, poured into saturated solution of sodium chloride. The green solid was filtered and collected. The crude product was recrystallized from ethanol. Green powder of **3d** (0.98 g) was obtained in 25% yield. ^{1}H NMR (d_6-DMSO): δ1.71 (s, 12H, CH_3), 1.77 (t, 2H, J = 5.6 Hz, CH_2), 2.57 (t, 4H, J = 5.6 Hz, CH_2), 5.52 (s, 4H, NCH_2), 6.39 (d, 2H, J = 14.4 Hz, CH), 7.20–7.68 (m, 16H, Ar–H), 8.24 (d, 2H, J = 14.4 Hz, CH). High resolution MS, *m/z*: calc. 671.3005 $[M-Cl]^+$, measured 671.2994 $[M-Cl]^+$.

2.3.10. Dye 3e

2e (1.5 g, 4 mmol), 2-chloro-1-formyl-3-hydroxymethylene cyclohexene (0.344 g, 2 mmol) and sodium acetate (0.376 g, 4 mmol) were heated in 25 mL of acetic anhydride at 70 °C for 15 min. The green solution was cooled and, then, poured into saturated solution of sodium bromide. The green solid was filtered and collected. The crude product was recrystallized from acetone. Green powder of **3e** (0.51 g) was obtained in 27% yield. ^{1}H NMR ($CDCl_3$): δ 1.78 (s, 12H, CH_3), 1.78 (s, 2H, CH_2), 2.57 (s, 4H, CH_2), 5.77 (s, 4H, NCH_2), 6.28 (d, 2H, J = 14 Hz, CH), 7.11–7.44 (m, 8H, Ar–H), 7.55 (d, 4H, J = 8.4 Hz, Ar–H), 8.18 (d, 4H, J = 8.4 Hz, Ar–H), 8.28 (d, 2H, J = 14 Hz, CH). High resolution MS, *m/z*: calc. 725.2895 $[M-Br]^+$, measured 725.2863 $[M-Br]^+$.

3. Results and discussion

3.1. Synthesis of the dyes

Heptamethine 3*H*-indocyanine dyes had been deeply synthesized by Patonay and Narayanan [21] and Waggoner group [18]. We, also, have synthesized several NIR 3*H*-indocyanine dyes with different substituents on scaffold of the dyes and investigated the photostabilities of the dyes recently [15,22]. This paper reports the syntheses of several novel NIR 3*H*-indocyanine dyes with different groups on their nitrogen atoms of 3*H*-indolenines and investigates the effect of the substitution on the photostabilities. The synthesis routes were shown in Scheme 1. The dyes **3a**, **3c**–**3e** were synthesized through the different intermediate **2a**, **2c**–**2e** in acetic anhydride and purified by recrystallized from acetone or ethanol solvent efficiently. The dye **3b** was purified through column chromatography with higher yield. The carboxyl groups at the *N*-position of 3*H*-indolenines of **3a** and **3b** can be converted to their NHS-esters and reacted with amine-containing labels. Compared with **3b**, the novel **3a** bearing the carboxylbenzyl functional group at *N*-position of 3*H*-indolenine exhibits improved photostability and is favorable to be used as the labels of the biomolecules.

3.2. Spectra properties of the dyes in methanol

The substituents on nitrogen positions of the cyanine dyes affect the electronic properties of the dyes. Typical absorption and emission spectra are shown in Fig. 2. Generally, the shapes of the spectra are independent of the substituents, but their maxima are shifted. The spectra data are listed in Table 1. The absorption and emission spectra of dye **3a** show a red shift, large molar extinction coefficient, and large stokes shift because of the introducing of large benzyl group compared with dye **3b** with twistable carboxylpentyl group. Similarly, the dyes with electron-donating group (**3c** and **3f**) on *N*-position of 3*H*-indolenine exhibit the larger stokes shifts compared with the dyes with electron-withdrawing group (**3d** and **3e**). The fluorescence quantum yields of these dyes do not show much difference even in the case of **3e** with nitro group.

Table 1
Spectra properties of cyanine dyes in methanol solvent

Entry	$\lambda_{abs}/\lambda_{em}$ (nm)	Φ (in ethanol)	ε ($\times 10^5$ mol^{-1} cm^{-1} L)	Stokes shifts (nm)
3a	786/814	0.1097	2.5	29
3b	782/808	0.1188	2.3	26
3c	785/813	0.1315	2.2	28
3d	784/809	0.1484	2.2	25
3e	785/807	0.1009	2.2	22
3f	784/813	0.1168	2.3	29

3.3. Comparisons on the photofading of the dyes

An important requirement for the application of fluorescent dyes in fluorescence microscopy is the high photostability. To get a deeper insight into the relationship of structure and photostabilities of the NIR cyanine dyes, photofading behaviors of the dyes with different substitutions on *N*-position of 3*H*-indolenine were determined in ethanol solution. The photoreactions were carried out in quartz cells (1 cm in width) where sample solution was irradiated with a 500 W I-W lamp at room temperature. The results were shown in Fig. 3.

After irradiation of 6 h, the nitro-substituted dye **3e** had showed 100% photofading, but dye **3c** (methyl-substituted) and **3f** (R = H) had showed only 24% decrease in maximal absorbance. It can be obtained that photostabilities decrease in the series of **3f** > **3c** > **3d** > **3a** > **3b** > **3e** and all the other dyes except **3e** exhibit preferable photostability to the carboxylpentyl-substituted dye **3b**, which is well known in the labeling of biomolecules. These data show that the dyes with electron-donating group on nitrogen atom perform improved photostability compared with the dyes with electron-withdrawing group.

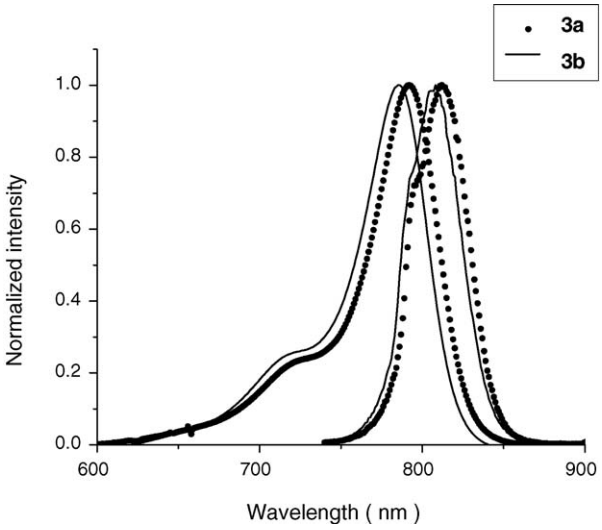

Fig. 2. Absorption and emission spectra of **3a** and **3b**.

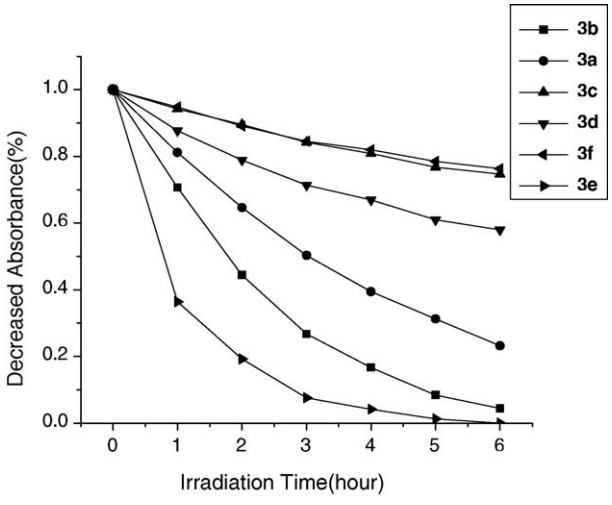

Fig. 3. Comparisons on the photofading of the NIR dyes.

3.4. Rate constants of photoreaction

Based on the mechanism of photoreaction, the equation of photoreaction is shown as below:

$$-\frac{\mathrm{d[Dye]}}{\mathrm{d}t} = k_1[\mathrm{Dye}][\mathrm{O_2}] \quad (1)$$

As a constant, the concentration of O_2 in the solution full of oxygen is about 3×10^{-4} mol/L [23]. So the formula is as follows:

$$-\frac{\mathrm{d[Dye]}}{\mathrm{d}t} = k[\mathrm{Dye}] \quad (2)$$

$$\ln \frac{[\mathrm{Dye}]_0}{[\mathrm{Dye}]_t} = kt \quad (3)$$

$[\mathrm{Dye}]_0$ is the initial concentration of the dye, $[\mathrm{Dye}]_t$ is the concentration of the dye after the irradiation of t min. Based on Beer rule, it has the linear relation between the concentration of the dye and the absorbance in maximal wavelength for the low concentration dye. So the formula is as follows:

$$\ln\left(\frac{A_0}{A_t}\right) = kt \quad (4)$$

A_0 is the absorbance in maximal wavelength before the irradiation, and A_t is the absorbance in maximal wavelength after the irradiation. The slope of the line k is the speed constant of the photodegradation reaction [24]. Therefore, the rate constants of the photodegradation reaction were obtained from the experimental tests, respectively. The rate of the photodegradation of the nitro-substituted dye **3e** was 10 times larger than that of the fluoro-substituted dye **3d**, and 20 times larger than that of the methyl-substituted dye **3c**. The rate constants of photoreaction based on the experiments were shown in Table 2.

3.5. Comparisons of the redox potentials of the dyes

Cyclic voltammetry (CV) is an electrochemical method determining the extent of the redox reaction. It is well known that the oxidation of the cyanine dye is the reaction of losing electron and, then, combining with oxygen. Lenhard and Cameron had investigated the substitution effect in the polymethine chain of cyanine dyes on the stability of the radicals during the electro-redox reaction of the dyes [25]. However, few works had been done about the photostabilities of the NIR cyanine with different *N*-position substitution.

Table 2
The rate constants of photofading and the redox potentials of the dyes in CH_3CN in scan rate of 100 mV/s

Entry	Rate constants k ($\times 10^{-3}$ mol min^{-1})	E_{ox1} (V)	E_{ox2} (V)
3a	4.04	0.404[a]	–
3b	8.70	0.298	–
3c	0.825	0.368	1.079
3d	1.51	0.382	1.019
3e	13.9	0.411	–
3f	0.756	0.368	1.143

[a] The redox potential obtained was not very precise because of the bad solubility in CH_3CN.

The electron-withdrawing group (NO_2, CF_3SO_2) on the benzene of π-conjugated moiety will enhance the stability of the cyanine dyes [9]. The main reason is that the electron-withdrawing group would enlarge the π-conjugated system and decrease the density of the electron cloud on the π-conjugated system. Therefore, the oxidation on the methine chains is not easy to take place.

However, the substitution on *N*-position of 3*H*-indolenine rings is contrary to the above results and explanations. The nitro-substituted cyanine dye on the side chain exhibits poor stability and the irreversible cyclic voltammetry (Fig. 4), where one-electron oxidation of the cationic cyanine dye yields the corresponding radical dication.

Fig. 4 shows the difference of the CV curves between the typical **3e** with electron-withdrawing group (NO_2) and **3c** with electron-donating group (CH_3) in CH_3CN/$TBAPF_6$ using potential scan rate 100 mV/s is obvious. The single-electron redox reaction of **3e**, labeled peak I, is found to be chemically irreversible, and the peak potential about 0.411 V versus Ag/Ag^+ is higher than that of **3c** (0.368 V), which attributes to the tendency of the reduced electron intensity on the conjugated methine chain induced by the large π planar structure of nitrobenzyl group. However, the first electron oxidation process (0.368 V versus Ag/Ag^+) of **3c** is reversible. The second-electron oxidation of **3c**, labeled peak II, occurs at 1.079 V, but no clear voltammetric peak was observed for the dye **3e**. These data imply that one electron oxidation might make **3e** decomposed and **3c** is tolerable to the oxidation with a reversible recovery. The cyclic

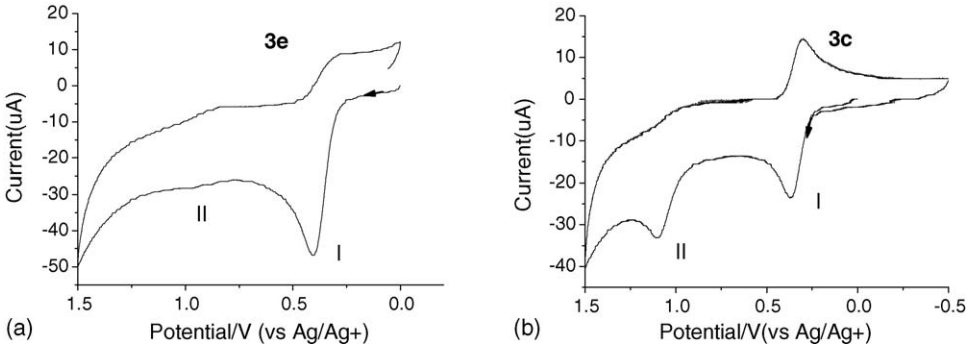

Fig. 4. Cyclic voltammetry curves of the dyes **3e** (NO_2) and **3c** (CH_3) with scan rate of 100 mV/s.

voltammetry of **3b**, with poor photostability, is similar to that of **3e**, and those of the dyes with fair photostability, **3f**, **3d** and **3a**, are similar to that of **3c**.

The N–CH_2 group affects electron density of the large π-conjugated planar structure of the dyes with hyperconjugation. One-electron oxidation produces the dication radicals of dyes, which lead to the molecules of the dye more "positive" and electrophilic. An electron-donating group linked with the N–CH_2 might make the "reactive" dye less electrophilic by electron delocalization. On the other side, electron-withdrawing group such as nitro results in the dication more reactive and instable.

Different from the other dyes, the electron-withdrawing effect of the carboxyl group for the dye **3b** was weak due to the distance of the long alkyl chain. Therefore, the electronic effect was not the main factor led to the photofading. The one-electron oxidation potential of **3b** was at 0.298 V and lower than those of the other dyes, indicating that the higher HOMO resulted in the higher oxidation activity.

3.6. Mechanism of the photofading

As is well known, there are two possible mechanisms of the interaction of an excited dye molecule and dioxygen, which lead to the formation of singlet oxygen ($^1O_2$) and superoxide anion (O_2^-), respectively [26] (Fig. 5). It has been proved that both singlet oxygen ($^1O_2$) and superoxide (O_2^-) contribute to the photofading of polymethine cyanine dyes [27].

Parallel experiments were carried out in methanol and deuterated methanol solution of dye **3c**. Fig. 6 shows the changes of the maximal absorbance of dye **3c** in methanol compared with that in deuterated methanol. After 5 h of irradiation, dye **3c** in methanol had showed 15% fading, but dye **3c** in deuterated methanol had showed 63% fading. The rate constant of the later was 6.2 times larger than that of the former, but the lifetime of singlet oxygen in deuterated methanol is 20 times larger than that in methanol [28]. If the photodegradation of **3c** proceeds by the singlet oxygen mechanism alone, the observed rate constant in methanol should be 20 times larger than that in methanol. Therefore, singlet oxygen and superoxide anion all affect the dye's photobleaching.

The final residue from the decomposition of the dyes showed the regular oxidized product peaks (m/z (+) of $[M+H]^+$, **3c**: 266, **3e**: 297, **3d**: 270) by HPLC–MS with API–ES ionization. That means the mechanism of photoreaction assembles well with the reaction in Fig. 7, although the products of the dyes decay have not yet been isolated and structurally characterized. And the available HPLC–MS data are consistent with the

Mechanism 1:

$$\text{Dye} + h\nu \longrightarrow {}^1\text{Dye}^* \xrightarrow[\text{crossing}]{\text{intersystem}} {}^3\text{Dye}^* \quad (1)$$

$${}^3\text{Dye}^* + {}^3O_2 \longrightarrow \text{Dye} + {}^1O_2 \quad (2)$$

$$\text{Dye} + {}^1O_2 \longrightarrow \text{Photofading} \quad (3)$$

Mechanism 2:

$$\text{Dye} + h\nu \longrightarrow {}^1\text{Dye}^* \quad (1)$$

$${}^1\text{Dye}^* + O_2 \longrightarrow \text{Dye}^{\ddagger\cdot} + O_2^{\cdot-} \quad (2)$$

$$\text{Dye} + O_2^{\cdot-} \longrightarrow \text{Photofading} \quad (3)$$

Fig. 5. Mechanisms of dye photofading.

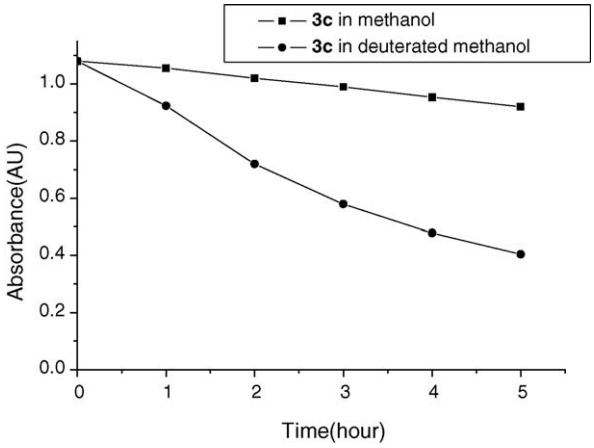

Fig. 6. Photofading of **3c** in methanol and the deuterated methanol.

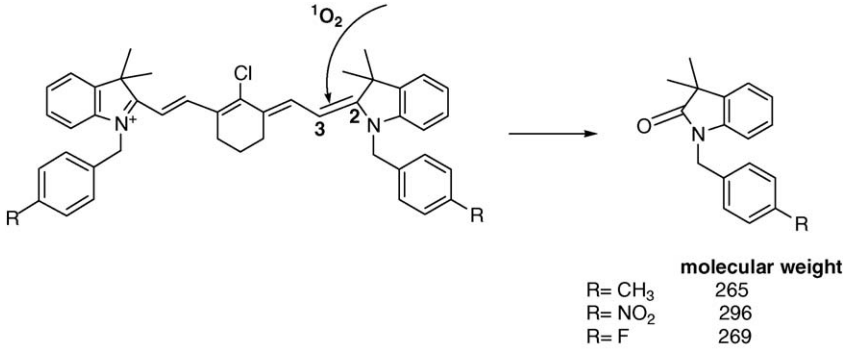

Fig. 7. Photoreaction of the NIR dyes induced by the singlet oxygen.

similar decomposition pathway of the heptamethine cyanine that depicted in the previous literature [29].

4. Conclusion

In summary, we have synthesized serials of novel NIR 3*H*-indocyanine dyes to investigate the relationship between the structure and the photostability. The carboxylbenzyl-*N*-substituted dye **3a** shows improved photostability compared with the well-known carboxylpentyl-*N*-substituted dye **3b**, which may be the effect of large aromatic ring on the nitrogen atoms. The electron-withdrawing group at N-atom of 3*H*-indolenine influences the photostability of the dyes negatively, but electron-donating group is favorable. The effects of substitution on photostability for several different substitutions on the *N*-positions decrease in the series: **3f**, **3c** > **3d** > **3a** > **3b** > **3e**. It is worthwhile to design novel cyanine dyes with good photostability for the potential imaging application in biosystem.

Acknowledgements

This work was financially supported by the Education Ministry of China and the National Natural Science Foundation of China (project nos. 20128005, 20376010 and 20472012).

References

[1] V. Ntziachristos, R. Weissleder, Opt. Lett. 26 (2001) 893–895.
[2] V. Ntziachristos, J. Ripoll, R. Weissleder, Opt. Lett. 27 (2002) 333–335.
[3] R. Weissleder, V. Ntziachristos, Nat. Med. 9 (2003) 123–128.
[4] W.K. Moon, Y. Lin, T. O'Loughlin, Y. Tang, D.E. Kim, R. Weissleder, C.H. Tung, Bioconjugate Chem. 14 (2003) 539–545.
[5] W. Pham, W.F. Lai, R. Weissleder, C.H. Tung, Bioconjugate Chem. 14 (2003) 1048–1051.
[6] D.B. Shealy, M. Lipowska, J. Lipowski, N. Narayanan, S. Sutter, I. Strekowski, G. Patonay, Anal. Chem. 67 (1995) 247–251.
[7] Y. Ye, S. Bloch, S. Achilefu, J. Am. Chem. Soc. 126 (2004) 7740–7741.
[8] M. Lipowska, G. Patonay, L. Strekowski, Synthetic Commun. 23 (1993) 3087–3094.
[9] S. Murphy, G.B. Schuster, J. Phys. Chem. 99 (1995) 8516–8518.
[10] R. Guether, M.V. Reddington, Tethahedron Lett. 38 (1997) 6167–6170.
[11] B.R. Renikuntla, H.C. Rose, J. Eldo, A.S. Waggoner, B.A. Armitage, Org. Lett. 6 (2004) 909–912.
[12] O. Mader, K. Reiner, H.J. Egelhaaf, R. Fischer, R. Brock, Bioconjugate Chem. 15 (2004) 70–78.
[13] L. Tarazi, A. George, G. Patonay, L. Strekowski, Talanta 46 (1998) 1413–1424.
[14] T. Gorecki, G. Patonay, L. Strekowski, R. Chin, N. Salazar, J. Heterocycl. Chem. 33 (1996) 1871–1876.
[15] F. Song, X. Peng, E. Lu, R. Zhang, X. Chen, B. Song, J. Photochem. Photobiol. A: Chem. 168 (2004) 53–57.
[16] R.C. Benson, H. Kues, J. Chem. Eng. Data 22 (1997) 379.
[17] S. Fery-Forgues, D. Lavabre, J. Chem. Edu. 76 (1999) 1260–1264.
[18] R.B. Mujumdar, L.A. Ernst, S.R. Mujumdar, C.J. Lewis, A.S. Waggoner, Bioconjugate Chem. 4 (1993) 105–111.
[19] D.L. Gallaher Jr., Johnson, M.E. Johnson, Analyst 124 (1999) 1541.
[20] X. Chen, Z.G. Yao, Chem. J. Chin. Univ. 17 (1996) 1613–1616.
[21] N. Narayanan, G. Patonay, J. Org. Chem. 60 (1995) 2391.
[22] L. Wang, X. Peng, F. Song, Er. Lu, J. Cui, X. Gao, R. Lu, Dyes Pigments 61 (2004) 103–107.
[23] W. Rettig, B. Strehmel, S. Schrader, et al., Applied Fluorescence in Chemistry. Biology and Medicine [M], Springer, Berlin, 1999, p. 1932240.
[24] C. Ping, S. Shuqing, H. Yunfeng, Q. Zhiguo, Z. Deshui, Dyes Pigments 41 (1999) 227–231.
[25] J.R. Lenhard, A.D. Cameron, J. Phys. Chem. 97 (1993) 4916–4925.
[26] C.P. Chen, B.M. Zhou, D.H. Lu, G.Z. Xu, J. Photochem. Photobiol. A: Chem. 89 (1995) 25–29.
[27] J. Li, P. Chen, J. Zhao, D.S. Zheng, T. Okazaki, M. Hayami, Photogr. Sci. Photochem. 15 (1997) 343.
[28] M.A.J. Rodgers, J. Am. Chem. Soc. 105 (1983) 6201–6205.
[29] P. Chen, J. Li, et al., Dyes Pigments 37 (1998) 213–222.